



Influence of jarosite precipitation on iron balance in heap bioleaching at Monywa copper mine

KYAW MIN SOE^{1,2,3}, RENMAN RUAN^{1,2,5}, YAN JIA^{1,2,5}, QIAOYI TAN^{1,2,5}, ZHENTANG WANG⁴,
JIANFENG SHI⁴, CHUANGANG ZHONG⁴, HEYUN SUN^{1,2,5}✉

¹ CAS Key Laboratory of Green Process and Engineering, Institute of Process Engineering, Chinese Academy of Sciences, Beijing, People's Republic of China

² National Engineering Laboratory for Hydrometallurgical Cleaner Production Technology, Chinese Academy of Sciences, Beijing, People's Republic of China

³ University of Chinese Academy of Sciences, Beijing, People's Republic of China

⁴ Wanbao Mining Ltd, Beijing, People's Republic of China

⁵ State Key Laboratory of Biochemical Engineering Institute of Process Engineering, Chinese Academy of Sciences, Beijing, People's Republic of China

How to cite this article: Kyaw Min Soe, Renman Ruan, Yan Jia, Qiaoyi Tan, Zhentang Wang, Jianfeng Shi, Chuangang Zhong, Heyun Sun. Influence of jarosite precipitation on iron balance in heap bioleaching at Monywa copper mine. Journal of Mining Institute. 2021. Vol. 247, p. 102-113. DOI: 10.31897/PMI.2021.1.11

Abstract. Ferric iron is an important oxidant in sulfide ore bioleaching. However, recirculating leach liquors leads to excess iron accumulation, which interferes with leaching kinetics and downstream metal recovery. We developed a method for controlling iron precipitation as jarosite to reduce excess iron in heap bioleaching at Monywa copper mine. Jarosite precipitation was first simulated and then confirmed using batch column tests. From the simulations, the minimum pH values for precipitation of potassium jarosite, hydronium jarosite, and natrojarosite at 25 °C are 1.4, 1.6, and 2.7, respectively; the minimum concentrations of potassium, sulfate, ferric, and sodium ions are 1 mM, 0.54, 1.1, and 3.2 M, respectively, at 25 °C and pH 1.23. Column tests indicate that potassium jarosite precipitation is preferential over natrojarosite. Moreover, decreased acidity (from 12 to 8 g/L), increased temperature (from 30 to 60 °C), and increased potassium ion concentration (from 0 to 5 g/L) increase jarosite precipitation efficiency by 10, 5, and 6 times, respectively. Jarosite precipitation is optimized by increasing the irrigating solution pH to 1.6. This approach is expected to reduce the operating cost of heap bioleaching by minimizing the chemicals needed for neutralization, avoiding the need for tailing pond construction, and increasing copper recovery.

Key words: jarosite precipitation; thermodynamics; column bioleaching; iron balance; Monywa copper mine

Acknowledgement. This research was supported by the National Natural Science Foundation of China General Projects (N 51674231), the Innovation Academy for Green Manufacture at the Chinese Academy of Sciences (IAGM-2019A08), and the Key Research Program of the Chinese Academy of Sciences (N ZDRW-ZS-2018-1).

Introduction. Monywa copper mine (Myanmar) is the second-largest source of copper in Southeast Asia; the main copper-bearing mineral is chalcocite (Cu₂S), which is acid-soluble and amenable to bioleaching [18, 20, 32]. The pyrite (FeS₂) content in the ore is relatively high, with an average of approximately 13 % [7, 15]. Pyrite oxidation generates sulfuric acid and soluble iron; owing to solution recirculation, this results in increased acid and iron concentration in the leach solution over time [5]. This increase in the iron concentration of the solution decreases the efficiency and stability of copper recovery through electrowinning [13, 23], hindering the achievement of the target output [9]. In particular, an increase in the ferric iron concentration of the pregnant leach solution (PLS) affects the selectivity of solvent extraction [27, 30, 31]. Moreover, excess iron has been reported to decrease current efficiency, increase energy consumption, and change the surface morphology of cathodic copper in electrowinning. Excess iron is typically removed by bleeding copper-bearing electrolyte to waste and replacing it with sulfuric acid [29]. Alkaline substances (e.g., Ca(OH)₂ and NaOH) are generally used to neutralize the bled acidic iron-rich solution, and ferric iron is precipitated as ferric hydroxide, which is pressed and filtered to dry pile or stored in tailings ponds [16]. In the Zijinshan copper mine, excess acidic ferric solution is neutralized by lime, which costs more than 1000 USD per ton of copper [17, 19]. The dewatering of ferric hydroxide is difficult, and therefore the storage of precipitates requires large areas. The high ionic strength of the



PLS solution increases the consumption of neutralization chemicals and results in the formation of hard-to-filter colloidal substances [19].

The precipitation of jarosite [with a generic formula of $AFe_3(SO_4)_2(OH)_6$, where A is a monovalent cation such as K^+ , Na^+ , NH_4^+ or H_3O^+] is widely used in the hydrometallurgical industry to remove iron, sulfate, and alkali metals. The advantages of jarosite precipitation include good filterability and settleability of the precipitates, with minor losses of valuable divalent metals [2, 10, 11]. In heap leaching systems, the formation of secondary iron minerals, such as jarosite, is widespread [3, 8]. Jarosite is deposited in the ore heap, resulting in a reduction in the ferric iron concentration of the leach liquor [6, 28]. The removal of excess iron through jarosite instead of hydroxide precipitation could reduce the cost of chemicals used for acid neutralization [12]. To this end, control over jarosite precipitation during heap bioleaching is important; however, the conditions that promote jarosite precipitation during heap bioleaching are not fully understood. In this study, we investigated the key factors that influence jarosite precipitation kinetics in heap bioleaching of copper sulfide ore from the Monywa copper mine. The primary aim of this work is to facilitate a process to remove excess iron through jarosite precipitation. Column experiments were used to simulate heap bioleaching conditions.

Materials and methods. Ore and solution samples. Column experiments were conducted with low-grade copper sulfide ore from the Monywa copper mine. The ore had a particle size of P80 (80 % passing) 10 mM. The contents of the main elements in the ore samples were analyzed using previously described methods [25] (Table 1). The average pyrite content is 14.6 %.

Table 1

Elemental abundances of major ore sample components

Ore sample	Elemental content, wt. %			
	Cu	CNsCu*	Fe	S
I	0.24	0.23	6.87	–
II	0.54	0.52	7.71	9.24
III	0.48	0.43	7.84	9.41
IV	0.44	0.42	5.02	–

Note. * CNsCu – copper extracted by cyanide solvent.

Raffinates, the solution after copper extraction, and intermediate leach solution (ILS) were collected from the copper production system; their chemical compositions are summarized in Table 2. Chemical composition of intermediate leach solution: Redox (vs. Ag/AgCl) 526 mV; pH 1.23. Elemental content, g/L: Fe 31.35; Cu 2.42; Ca 0.51; Mg 4.15; K 0.0039; Na 0.087; Al 12.78; Mn 1.73; SO_4^{2-} 157.44; Cl^- 2.26. Redox potentials of the raffinate samples were 493-553 mV (vs. Ag/AgCl), and pH values ranged from 0.99 to 1.67. The highest iron concentration in raffinate samples was 40 g/L; the sulfate concentration reached 157 g/L in the ILS. The ionic strength of the ILS solution was calculated to be approximately 8.5 mol/kg. However, the concentrations of potassium and sodium were very low, which is unfavourable for potassium and sodium jarosite precipitation. The thermodynamics of jarosite precipitation were simulated based on the ILS properties using the Medusa software (Royal Institute of Technology, Sweden) [33].

Table 2

Chemical composition of raffinates

Raffinate sample	Redox vs. Ag/AgCl, mV	pH	Elemental content, g/L				
			Cu	Fe	Fe ²⁺	Fe ³⁺	Acid
I	553	1.23	0.95	32.08	1.21	30.87	10.28
II	497	0.99	0.79	18.27	1.26	17.01	18.53
III	493	1.38	1.26	40.32	4.45	35.87	12.35
IV	534	1.67	1.34	36.99	1.50	35.49	11.32

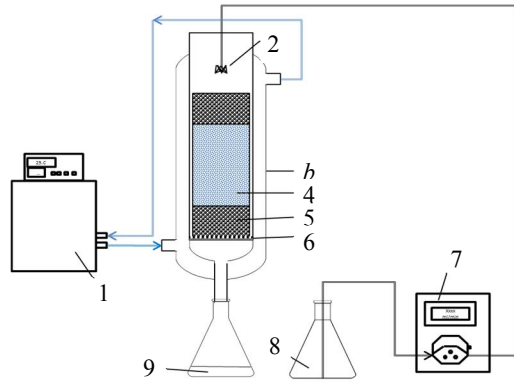


Fig.1. Schematic diagram of the experimental set-up

1 – water bath; 2 – dripper; 3 – water jacket; 4 – ore sample;
5 – cobblestone; 6 – pedestal; 7 – peristaltic pump; 8 – feed solution; 9 – pregnant leach solution

Jarosite precipitation column tests. Column leaching tests were conducted to simulate jarosite precipitation in heap bioleaching. The experimental set-up is shown in Figure 1. The glass columns were 20 cm high and 5 cm in diameter. The temperature of the columns was controlled with an isothermal circulating water bath system. Each column was filled with 600 g of ore irrigated with raffinate at a flow rate of 0.2 mL/min. Jarosite precipitation tests were conducted under various operating conditions, using different monovalent cations (Na^+ , K^+), reaction temperatures 30-60 °C, solution acidities 8-16 g/L, and K^+ concentrations 0-5 g/L (Table 3). Irrigation solutions with monovalent cations (Na^+ or K^+) were prepared by adding sodium sulfate, potassium sulfate, or potassium chloride into the raffinate. The acidity of the irrigation solution was adjusted by adding calcium carbonate or sulfuric acid.

Table 3

Column test experimental conditions

Column	Ore sample	Raffinat solution sample	Irrigation solution				Temperature, °C
			Na^+ , g/L	K^+ , g/L	pH	Acidity, g/L	
1	I	I	2	–	1.23	10.3	35
2	I	I	–	2	1.23	10.3	35
3	I	I	–	–	1.23	10.3	35
4	II	II	–	–	0.99	18.5	30
5	II	II	–	–	0.99	18.5	45
6	II	II	–	–	0.99	18.5	60
7	III	III	–	2	1.43	8	27
8	III	III	–	2	1.38	12	27
9	III	III	–	2	1.32	16	27
10	IV	IV	–	0	1.67	11.3	27
11	IV	IV	–	1	1.67	11.3	27
12	IV	IV	–	5	1.67	11.3	27

During all experiments, solution samples were collected daily from the pregnant leach solution containers for analysis. The redox potential of the solution was measured using a platinum ring electrode with a combined Ag/AgCl reference electrode (3 M KCl); pH was determined using pH meter (SevenGo Pro, Mettler Toledo, Switzerland). The acidity and the concentration of the Fe^{2+} were determined by titration with sodium hydroxide (NaOH) and potassium dichromate ($\text{K}_2\text{Cr}_2\text{O}_7$) solution, respectively. The concentrations of soluble total Fe (TFe), Cu^{2+} , K^+ , and Na^+ were measured by atomic absorption spectrophotometer (AAS). Soluble sulfur was measured by C.S. Analyzer (HSC, Keguo, China). After completion of leaching, ore residues were washed with a 5 g/L sulfuric acid solution, unloaded from the column, and dried in an oven at 50 °C. The dried residues were crushed and ground to $< 74 \mu\text{m}$ and analyzed for Cu, Fe, S, S^{2-} , K, and Na as previously described [25]. Copper leaching yields were calculated based on the volume and concentration in the feed solution and leachate: $P = C_{\text{leachate}} V_{\text{leachate}} - C_{\text{feed}} V_{\text{feed}}$, where P – production; C_{leachate} – concentration in the leachate; V_{leachate} – volume of the leachate; C_{feed} – concentration in the feed solution; V_{feed} – volume of the feed solution.



Total copper, iron, and acid production during bioleaching was measured as the amount of their daily production. If production had a negative value, it was considered net consumption of copper, iron, and acid.

Results and discussion. Thermodynamic simulations of jarosite precipitation. The thermodynamics of jarosite precipitation were simulated based on the properties of the ILS. As the pH of the ILS solution was less than 2, the precipitation of iron hydroxide was ignored [4]. The possible chemical reactions of ferric iron in the leaching system are shown in Table 4. The results of reaction equilibrium calculations are shown in Fig.2, *a*, highlighting the effect of pH on jarosite precipitation. The minimum pH at which jarosite precipitation occurs differs notably for different monovalent cations. At a temperature of 25 °C, potassium jarosite precipitates at pH of ≥ 1.4 , whereas hydronium jarosite precipitation only occurs at pH values of more than 1.6; the minimum pH for natrojarosite precipitation is 2.7. Hence, the precipitation of potassium jarosite is expected at lower pH, and that of hydronium jarosite and then natrojarosite is expected to increase with increasing pH. Our results are consistent with those of past studies [1, 2]. Moreover, a preference for potassium jarosite is expected because the Gibbs free energy of formation follows the order $K^+ > Na^+ > H_3O^+ > NH_4^+$ [14].

Given the precipitation pH values of potassium jarosite, hydronium jarosite, and natrojarosite in ILS solution at 25 °C described above, our thermodynamic modelling indicated that no jarosite could form from ILS solution at 25 °C given the low pH of 1.23. Owing to the low concentration of potassium and sodium in the ILS, hydronium jarosite would likely become the dominant jarosite as pH is increased above 1.6 (Fig.2, *b*). The formation of hydronium jarosite would reduce the concentration of iron and produce acid.

Table 4

Chemical reactions in a $Fe^{3+}-M-SO_4^{2-}-H_2O$ system ($M = K^+, Na^+, NH_4^+, H_3O^+$) [22]

Chemical reaction	Log K
$Fe^{3+} + 2H_2O \rightleftharpoons 2H^+ + Fe(OH)_2^+$	-5.67
$Fe^{3+} + 3H_2O \rightleftharpoons 3H^+ + Fe(OH)_3$	-12.56
$Fe^{3+} + 4H_2O \rightleftharpoons 4H^+ + Fe(OH)_4^{2+}$	-21.6
$Fe^{3+} + 2SO_4^{2-} \rightleftharpoons Fe(SO_4)_2^-$	5.38
$2Fe^{3+} + 2H_2O \rightleftharpoons 2H^+ + Fe_2(OH)_2^{4+}$	2.95
$3Fe^{3+} + 4H_2O \rightleftharpoons 4H^+ + Fe_3(OH)_4^{5+}$	-6.3
$H^+ + Fe^{3+} + SO_4^{2-} \rightleftharpoons FeHSO_4^{2+}$	4.468
$Fe^{3+} + H_2O \rightleftharpoons H^+ + FeOH^{2+}$	-2.19
$Fe^{3+} + SO_4^{2-} \rightleftharpoons FeSO_4^+$	4.04
$2H^+ + SO_4^{2-} \rightleftharpoons H_2SO_4$	0.0
$H^+ + SO_4^{2-} \rightleftharpoons HSO_4^-$	1.98
$K^+ + H_2O \rightleftharpoons H^+ + KOH$	-14.46
$K^+ + SO_4^{2-} \rightleftharpoons KSO_4^-$	0.85
$Na^+ + H_2O \rightleftharpoons H^+ + NaOH$	-14.18
$Na^+ + SO_4^{2-} \rightleftharpoons NaSO_4^-$	0.7
$H_2O \rightleftharpoons H^+ + OH^-$	-14.0
$3Fe^{3+} + 2SO_4^{2-} + 7H_2O \rightleftharpoons 5H^+ + H_3OFe_3(SO_4)_2(OH)_6(s)$	5.39
$K^+ + 3Fe^{3+} + 2SO_4^{2-} + 6H_2O \rightleftharpoons 6H^+ + KFe_3(SO_4)_2(OH)_6(s)$	9.21

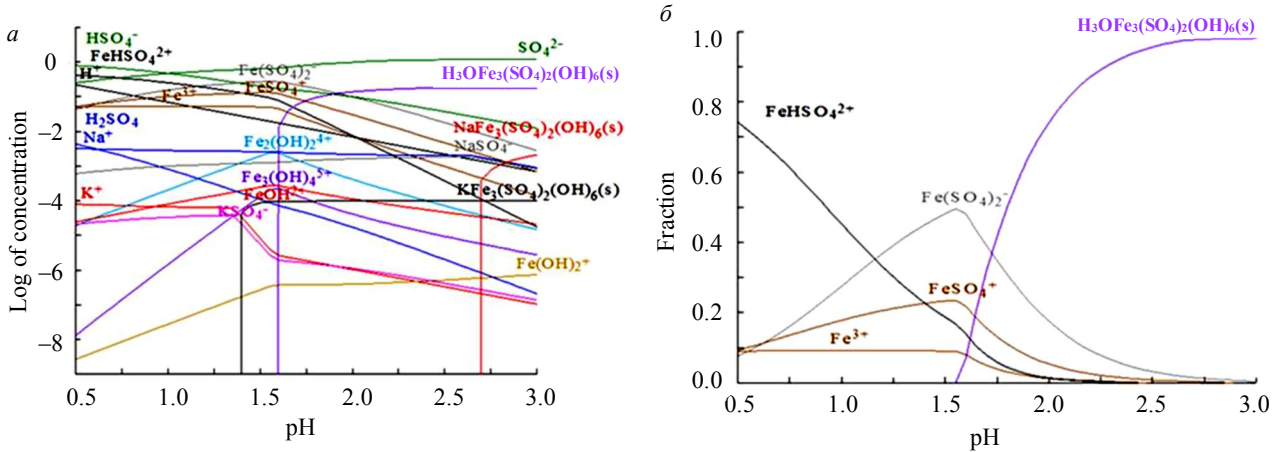


Fig.2. Logarithm of equilibrium concentration (a) and distribution (b) of ferric species in an Fe^{3+} -M- SO_4^{2-} - H_2O system as a function of pH of the intermediate leach solution.

Solution parameters: I = 8,5 mol/kg; Fe^{3+} = 0,56 mol/L; SO_4^{2-} = 1,6 mol/L; K^+ = 0,1 mmol/L; Na^+ = 3,8 mmol/L; t = 25 °C

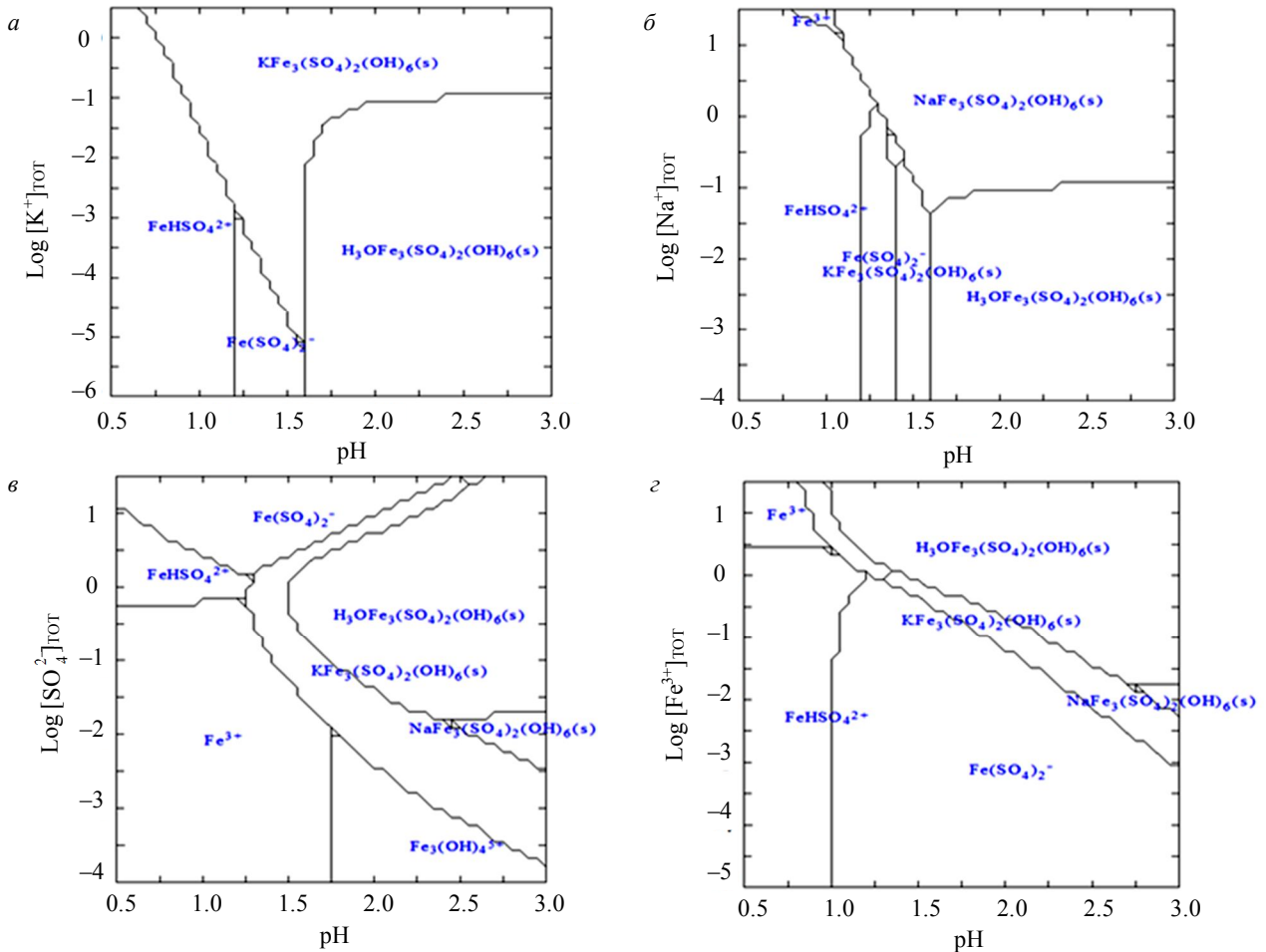
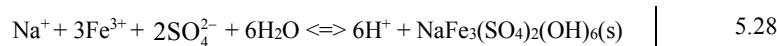


Fig.3. Predominant area diagrams of a Fe^{3+} -M- SO_4^{2-} - H_2O system as functions of pH and logarithmic concentrations of K^+ (a), Na^+ (b), SO_4^{2-} (c), and Fe^{3+} (d) of ILS



Predominant area diagrams of the Fe^{3+} -M- SO_4^{2-} - H_2O system as functions of pH and concentrations of K^+ , Na^+ , Fe^{3+} and SO_4^{2-} are shown in Fig.3. From Fig.3, a, potassium jarosite can form in



ILS if the concentration of K^+ increases to 1 mM (mmol/L). The minimum pH values for potassium jarosite and natrojarosite precipitation decrease as the concentrations of K^+ and Na^+ increase, respectively (Fig.3, a, b). Under the pH condition of the ILS, natrojarosite can form if the concentration of Na^+ increases to 3.2 M (mol/L). If the pH of the ILS > 1.6 , only 44 mM of Na^+ is necessary to promote natrojarosite precipitation. Increasing the concentration of SO_4^{2-} can reduce the minimum pH for potassium jarosite, hydronium jarosite, and natrojarosite formation (Fig.3, c). However, when the concentration of SO_4^{2-} exceeds 0.54 M, the minimum pH values for potassium jarosite and hydronium jarosite formation increase with increasing SO_4^{2-} concentration. Hence, decreasing the SO_4^{2-} concentration from 1.6 M in the ILS to 0.54 M would promote potassium and hydronium jarosite formation. The minimum pH values of potassium jarosite, hydronium jarosite, and natrojarosite formation could be decreased by increasing the concentration of Fe^{3+} (Fig.3, d). Potassium and hydronium jarosites could form if the concentrations of Fe^{3+} in the ILS are increased to 1.1 and 2.1 M, respectively. However, this may not be suitable for production systems unless a highly selective extractant is developed.

The thermodynamic simulations show that the solution composition of the ILS can be adjusted to promote jarosite precipitation. Increasing the concentration of K^+ is an important factor to promote jarosite formation under high acidity conditions, which is beneficial for chalcocite dissolution. Promoting hydronium jarosite and natrojarosite precipitation would require increasing the ILS pH and neutralizing free acid. These thermodynamic simulations were conducted at 25 °C, but actual bioleaching heaps may have a temperature gradient [26]. Hence, future studies should consider the effect of temperature in thermodynamic simulations. Moreover, as ammonium may be present in some mine sites owing to the use of explosives or addition as a nutrient for bioleaching, the presence of ammonium in leach liquors and the potential for ammonium jarosite formation should be evaluated.

Effect of monovalent cations. The influence of monovalent cations (K^+ , Na^+) on jarosite formation was studied in column tests using sample I and raffinate I at pH 1.23 and 35 °C. The raffinate solution was amended with 2 g/L of K^+ (as potassium sulfate) or Na^+ (as sodium sulfate) before use to irrigate the columns. The third column without K^+ or Na^+ supplementation was used as a control. The precipitation rate of potassium jarosite was faster than that of natrojarosite according to iron consumption and acidity production (Fig.4, a). The consumption of K and Na ions was almost linear (Fig.4, b), indicating that the rate of potassium jarosite and natrojarosite precipitation did not notably decrease over time. However, the higher consumption of K ions compared with Na ions further

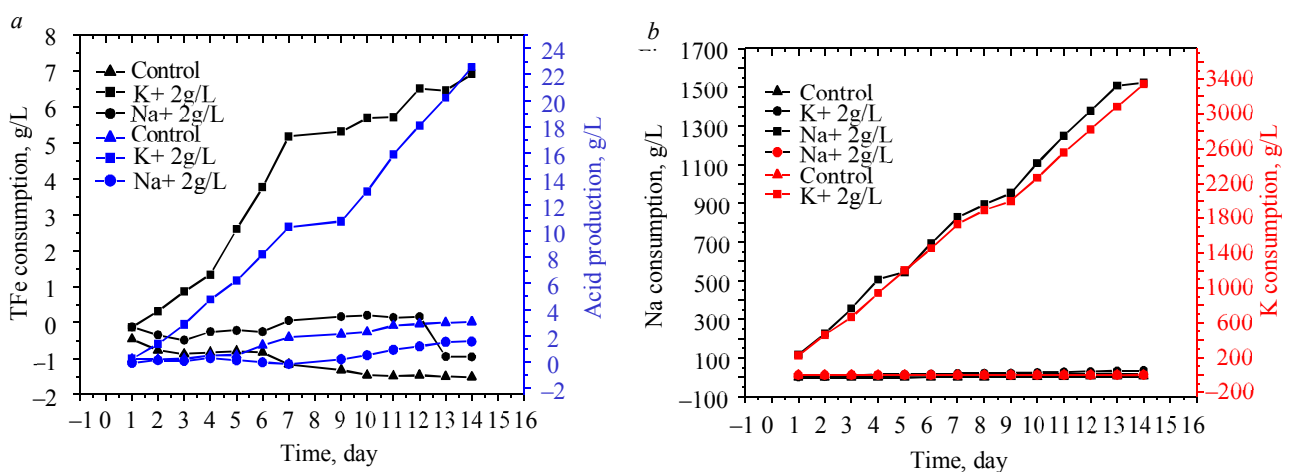
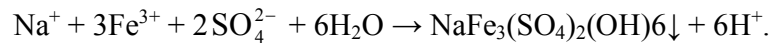


Fig.4. Total iron (TFe) consumption, acid production (a) and consumption (b) of Na^+ and K^+ as a function of time during column tests conducted with ore sample I and raffinate I at 35 °C in the absence of monovalent cation addition (control) and with Na^+ or K^+ supplementation



confirmed that the efficiency of potassium jarosite precipitation is higher than that of natrojarosite. The chemical reaction of natrojarosite precipitation is [21]:



According to the natrojarosite reaction, 1 g of sodium can precipitate approximately 7 g of iron and 8 g of sulfate as jarosite. For 1 g of potassium, the corresponding values are 4 g of iron and 5 g of sulfate.

The residue from the column with K^+ amended raffinate was more yellow than those from the Na^+ amended and control columns. Based on residue analysis (Table 5), the copper contents in residues from columns with monovalent cation-amended raffinates were lower, while total iron and reduced sulfur content were higher than in the control column. This indicates that the addition of K^+ and Na^+ promotes jarosite precipitation, not only removing excess iron and sulfate from the solution but also accelerating copper leaching from chalcocite and reducing the oxidation of pyrite.

Table 5

Chemical composition of residues and copper leaching

Test conditions	Residue weight, kg	Elemental content, %				Copper leaching, %
		Total Cu	Total Fe	Total sulfur	Reduced sulfur	
Control	0.589	0.14	4.74	11.70	8.89	40.0
Na^+ , 2 g/L	0.623	0.12	5.17	10.53	9.14	47.9
K^+ , 2 g/L	0.690	0.13	5.90	12.33	10.28	46.1

Effect of reaction temperature. The influence of temperature on jarosite formation was investigated with column tests using ore sample II and raffinate II (pH 0.99) at 30, 45, and 60 °C. The raffinate was not amended with any monovalent cations. The total soluble iron TFe consumption and acidity production during column leaching increased notably with increasing temperature (Fig.5, a). The residues formed at 45 and 60 °C were more yellow than those formed at 30 °C. Yellow precipitates were identified as potassium jarosite by X-ray diffraction (XRD) [25]. The results confirm that increase of temperature can promote jarosite precipitation.

Effect of acidity of solutions. The influence of acidity on jarosite formation was investigated through column experiments using ore sample III and raffinate III at 27 °C. The acidity of the irrigation solutions was adjusted to 8, 12, and 16 g/L by adding calcium carbonate and sulfuric acid. The irrigation solution was amended with 2 g/L K^+ (as potassium chloride). The acidity of the irrigation solution during the leaching process is shown in Fig.5, d. The results indicate that reducing the acidity of the irrigation solution enhances jarosite precipitation, as indicated by the increased consumption of total soluble iron and production of acid (Fig.5, b), which is consistent with a previous study [24]. Moreover, the concentration of potassium ion in the leaching solution under low acid conditions was notably lower than that under high acid conditions (Fig.5, d), and the consumption of K^+ increased with decreasing acidity (Table 6). The weights of all residues were higher than the original weight of the head ore as a result of jarosite accumulation in the columns. The weight was highest for the column operated at lower acidity (Table 7), which is consistent with the highest total soluble iron consumption (Fig.5, b). The contents of iron, sodium, and potassium in the residue were much higher than those in the raw ore, again indicating jarosite precipitation and accumulation in columns over time (Table 7). Sodium content of the residue was highest for the residue from the column operated at lowest acidity (8 g/L), indicating that low acidity is beneficial for natrojarosite

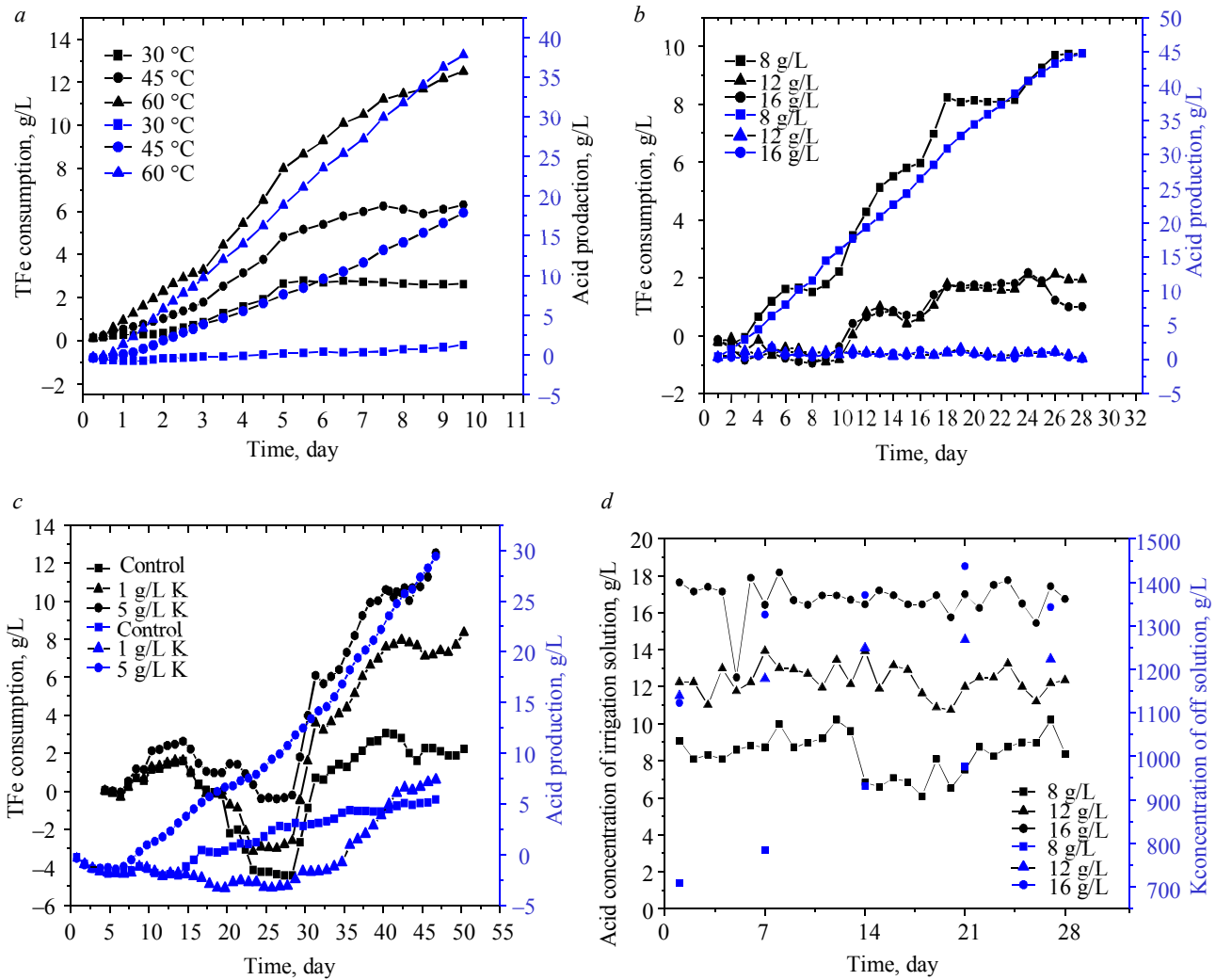


Fig.5. Total Fe (TFe) consumption and acid production as a function of time: during column tests conducted at different temperatures using ore sample II and raffinate II (a), during column leaching of ore III with raffinate III adjusted to three different acidities (b), during column leaching of ore sample IV with raffinate IV (c), and acidity of irrigation solutions during column leaching of ore III with raffinate III adjusted to three different acidities (d)

precipitation; the potassium content of the residue was highest for the residue from column operated at moderate acidity (12 g/L).

Table 6

Potassium ion consumption in solution after 28 days of column leaching of ore III with raffinate III adjusted to different acidities

Acidity, g/L	Average K concentration of leachate, mg/L	Total volume of leach solution, L	K ion consumption, g
8	844	8195	9.47
12	1211	8085	6.37
16	1320	7445	5.06

Table 7

Chemical compositions of head ore and residues after 28 days of column leaching of ore III with raffinate III adjusted to different acidities

Samples	Ore weight, g	Elemental content			
		Cu, %	Fe, %	Na, ppm	K, ppm
Head ore	600	0.48	7.84	793	1586
Leaching residue, g/L					



acidity 8	709	0.09	12.84	1083	6875
acidity 12	668	0.10	13.47	887	8875
acidity 16	686	0.08	11.66	923	3690

Effect of potassium ion concentration. The influence of K^+ concentration on jarosite formation was investigated through column experiments using sample IV and raffinate IV at 27 °C. The irrigation solution was amended with 0, 1, or 5 g/L K^+ (as potassium sulfate). Increasing potassium ion concentration resulted in increased consumption of total soluble iron and acid production (Fig.5, c). The weight of leaching residue with a particle size of less than 74 μm increased with increasing raffinate potassium ion concentration. The contents of iron, potassium, and total sulfur in the residue fraction with the particle size of less than 74 μm also increased with increasing raffinate potassium ion concentration, as shown in Table 8. This indicates that jarosite precipitation increases with increasing raffinate potassium ion concentration.

Table 8

Chemical compositions of residue with particle sizes of +74 μm and -74 μm after column leaching of ore sample IV with raffinate IV amended with 0 (control), 1, or 5 g/L K^+

K^+ supplementation to raffinate, g/L	Grain size, μm	Elemental content				
		Cu, %	Fe, %	K, ppm	S, %	S^{2-} , %
0	+74	0.05	5.38	0.1	8.19	7.88
	-74	0.05	4.12	0.03	6.05	5.24
1	+74	0.05	5.72	< 0.01	8.37	7.68
	-74	0.05	11.19	1.57	9.05	5.76
5	+74	0.06	7.27	0.45	9.02	7.55
	-74	0.05	11.19	3.16	10.55	5.28

Implication for heap bioleaching at Monywa copper mine. The results of this study show that the potential to remove iron from the ILS solution through jarosite formation is limited by the low concentration of monovalent cations. However, the addition of monovalent cations (Na and K) combined with the neutralization of free acid promotes potassium jarosite, hydronium jarosite, and natrojarosite formation to remove excess iron from the solution. We suggest that the addition of potassium ions is preferential because the formation of potassium jarosite occurs at lower pH values than those of hydronium jarosite and natrojarosite. When the acidity of the neutralization solution is high, the loss of copper ion can be ignored. However, at 25 °C and a pH of 1.5, Fe concentration of 49 g/L in the ILS is needed for the formation of potassium jarosite.

The stability of the jarosite depends on the acidity of the solution; however, the acidity of the leaching solution varies. Therefore, the use of a spent heap to facilitate iron removal through jarosite precipitation is suggested. This heap could be sealed after jarosite precipitation to ensure that jarosite is stably deposited. Small jarosite particles can adhere to the surfaces of large ore particles and deposits in pore spaces, reducing the porosity of the heap and reducing the oxygen availability. As a result, the activity of microbial ferrous iron oxidation is expected to decrease, leading to a reduction in the redox potential of the leaching solution. Using our proposed approach is expected to help with the balance of iron and acid in heap bioleaching at Monywa copper mine, reducing excess acid and iron release. This approach for optimizing iron and acid balance is expected to reduce the operating costs of heap bioleaching through the reduced cost of chemicals needed for neutralization, avoiding the need for constructing tailings ponds, and increased copper recovery.

Conclusions. The recirculation of leach liquors in heap bioleaching operations leads to the accumulation of excess iron, which interferes with leaching kinetics and downstream metal recovery. Jarosite formation has been proposed as an alternative approach for removing excess iron from



leach solutions, but the factors influencing jarosite formation in heap bioleaching are not fully understood. The present work investigated the key factors that influence jarosite precipitation kinetics in heap bioleaching of copper sulfide ore from the Monywa copper mine. Thermodynamic simulations indicate that solution acidity is a key factor affecting jarosite precipitation, and the minimum pH values for potassium jarosite, hydronium jarosite, and natrojarosite precipitation at 25 °C are 1.4, 1.6, and 2.7, respectively. Therefore, jarosite formation is not possible at 25 °C in ILS solution with a pH of 1.23. Moreover, thermodynamic simulations indicate that increasing the concentration of monovalent cations, iron, and sulfate promotes jarosite precipitation, especially under high acidity condition. Column tests show that decreasing acidity from 12 to 8 g/L, increasing temperature from 30 °C to 60 °C, and supplementing raffinate with potassium – all these increase jarosite precipitation. Column tests also show that potassium jarosite precipitates preferentially over natrojarosite under the study conditions. The results indicate that jarosite precipitation can be realized by increasing the concentration of Na⁺ and K⁺ and neutralizing free acid in raffinate.

Our results suggest that if jarosite precipitation is promoted in a spent heap, not only excess iron and sulfate would be removed from the solution, but that there would also be a reduction in pyrite oxidation and acid and iron release.

In conclusion, the present work provides new insight into optimizing iron and acidity balance in heap bioleaching operations, particularly at Monywa copper mine. Further work should explore actual temperature profiles in the bioheaps and use thermodynamic simulations to investigate the effect of temperature on jarosite precipitation. Moreover, the presence of ammonium in leach liquors and the potential for ammonium jarosite formation should be evaluated.

The authors gratefully acknowledged the support of the State Key Laboratory of Biochemical Engineering and Wanbao Mining Ltd. for help with sampling and experiments.

REFERENCES

1. Kaksonen A.H., Morris C., Rea S. et al. Biohydrometallurgical iron oxidation and precipitation: Part I – Effect of pH on process performance. *Hydrometallurgy*. 2014. Vol. 147-148, p. 255-263. DOI: 10.1016/j.hydromet.2014.04.016
2. Kaksonen A.H., Morris C., Rea S. et al. Biohydrometallurgical iron oxidation and precipitation. Part II: Jarosite precipitate characterisation and acid recovery by conversion to hematite. *Hydrometallurgy*. 2014. Vol. 147-148, p. 264-272. DOI: 10.1016/j.hydromet.2014.04.015
3. Davis-Belmar C.S., Cautivo D., Demergasso C., Rautenbach G. Bioleaching of copper secondary sulfide ore in the presence of chloride by means of inoculation with chloride-tolerant microbial culture. *Hydrometallurgy*. 2014. Vol. 150, p. 308-312. DOI: 10.1016/j.hydromet.2014.09.013
4. Brown J.B. Jarosite-geothite stabilities at 25 °C, 1 ATM. *Mineralium Deposita*. 1971. Vol. 6. Iss. 3, p. 245-252. DOI:10.1007/BF00208032
5. Jia Y., Sun H., Chen D. et al. Characterization of microbial community in industrial bioleaching heap of copper sulfide ore at Monywa mine, Myanmar. *Hydrometallurgy*. 2016. Vol.164, p. 355-361. DOI: 10.1016/j.hydromet.2016.07.007
6. Cogran P. Jarosite Reference Module in Earth Systems and Environmental Sciences. Elsevier Inc., 2018.
7. Zaw K., Swe Y., Myint T., Knight J. Copper deposits of Myanmar. *Memoirs*. 2017. Vol. 48, p. 573-588. DOI:10.1144/M48.26
8. Daoud J., Karamanev D. Formation of jarosite during Fe²⁺ oxidation by Acidithiobacillus ferrooxidans. *Minerals Engineering*. 2006. Vol. 19. Iss. 9, p. 960-967. DOI: 10.1016/j.mineng.2005.10.024
9. Demopoulos G.P., Gefvert D.L. Iron (III) Removal from Base-Metal Electrolyte-Solutions by Solvent-Extraction. *Hydrometallurgy*. 1984. Vol. 12. Iss. 3, p. 299-315. DOI: 10.1016/0304-386x(84)90003-3
10. Reyes I.A., Patiño F., Flores M.U. et al. Dissolution rates of jarosite-type compounds in H₂SO₄ medium: A kinetic analysis and its importance on the recovery of metal values from hydrometallurgical wastes. *Hydrometallurgy*. 2017. Vol. 167, p. 16-29. DOI: 10.1016/j.hydromet.2016.10.025
11. Dutrizac J.E., Hardy D.J., Chen T.T. The behaviour of cadmium during jarosite precipitation. *Hydrometallurgy*. 1996. Vol. 41. Iss. 2-3, p. 269-285. DOI: 10.1016/0304-386X(95)00062-L
12. Dutrizac J.E. The behaviour of the rare earths during the precipitation of sodium, potassium and lead jarosites. *Hydrometallurgy*. 2004. Vol. 73. Iss. 1-2, p. 11-30. DOI: 10.1016/j.hydromet.2003.07.009



13. Schlesinger M.E., King M.J., Sole K.C., Davenport W.G. Electrolytic Refining. Extractive Metallurgy of Copper. 5th edition. Oxford: Elsevier, 2011, p. 251-280.
14. Gaboreau S., Philippe V. Prediction of Gibbs free energies of formation of minerals of the alunite supergroup. *Geochimica Et Cosmochimica Acta*. 2004. Vol. 68. Iss. 16, p. 3307-3316. DOI: 10.1016/j.gca.2003.10.040
15. Mitchell A., Myint W., Lynn K. et al. Geology of the High Sulfidation Copper Deposits, Monywa Mine, Myanmar. *Resource Geology*. 2010. Vol. 61. Iss. 1, p. 29. DOI:10.1111/j.1751-3928.2010.00145.x
16. Havlík T. Leaching of Copper Sulphides // Hydrometallurgy. Woodhead Publishing, 2008, p. 341-443.
17. Jia Y., Ruan R., Zhong S. et al. Heap bioleaching of a net-acid generating copper sulfide: comparison of high and low acidity leaching systems. *Heap Leach Solutions*. 2015, p. 357-368.
18. Schlesinger M.E., King M.J., Sole K.C., Davenport W.G. Hydrometallurgical Copper Extraction: Introduction and Leaching. Extractive Metallurgy of Copper: 5th edition. Oxford: Elsevier, 2011, p. 281-322.
19. Ruan R., Liu X., Zou G. et al. Industrial practice of a distinct bioleaching system operated at low pH, high ferric concentration, elevated temperature and low redox potential for secondary copper sulfide. *Hydrometallurgy*. 2011. Vol. 108. Iss. 1, p. 130-135. DOI: 10.1016/j.hydromet.2011.03.008
20. Zaw K., Swe W., Barber A. et al. Introduction to the geology of Myanmar. *Memoirs*. 2017. Vol. 48, p.17. DOI:10.1144/M48.1
21. Das G.K., Acharya S., Anand S., Das R.P. Jarosites: A Review. *Mineral Processing and Extractive Metallurgy Review*. 1996. Vol. 16. Iss. 3, p. 185-210. DOI: 10.1080/08827509708914135
22. Jensen A.B., Webb C. Ferrous sulphate oxidation using thiobacillus ferrooxidans: a review. *Process Biochemistry*. 1995. Vol. 30. Iss. 3, p. 225-236. DOI: 10.1016/0032-9592(95)85003-1
23. Ghorbani Y., Becker M., Mainza A. et al. Large particle effects in chemical/biochemical heap leach processes – A review. *Minerals Engineering*. 2011. Vol. 24. Iss. 11, p. 1172-1184. DOI: 10.1016/j.mineng.2011.04.002
24. Leahy M.J., Schwarz M.P. Modelling jarosite precipitation in isothermal chalcopyrite bioleaching columns. *Hydrometallurgy*. 2009. Vol. 98. Iss. 1, p. 181-191. DOI: 10.1016/j.hydromet.2009.04.017
25. Y.Jia, H.-y.Sun, Q.-y.Tan et al. Linking leach chemistry and microbiology of low-grade copper ore bioleaching at different temperatures. *International Journal of Minerals, Metallurgy, and Materials*. 2018. Vol. 25. Iss. 3, p. 271-279. DOI: 10.1007/s12613-018-1570-2
26. Halinen A.-K., Beecroft N.J., Määttä K. et al. Microbial community dynamics during a demonstration-scale bioheap leaching operation. *Hydrometallurgy*. 2012. Vol. 125-126, p. 34-41. DOI: 10.1016/j.hydromet.2012.05.001
27. Quijada-Maldonado E., Romero J., Osorio I. Selective removal of iron (III) from synthetic copper (II) pregnant leach solutions using [bmim][Tf2N] as diluent and TFA as extracting agent. *Hydrometallurgy*. 2016. Vol. 159, p. 54-59. DOI: 10.1016/j.hydromet.2015.11.003
28. Gao K., Jiang M., Guo C. et al. Reductive dissolution of jarosite by a sulfate reducing bacterial community: Secondary mineralization and microflora development. *Science of the Total Environment*. 2019. Vol. 690, p. 1100-1109. DOI: 10.1016/j.scitotenv.2019.06.483
29. Izadi A., Mohebbi A., Amiri M., Izadi N. Removal of iron ions from industrial copper raffinate and electrowinning electrolyte solutions by chemical precipitation and ion exchange. *Minerals Engineering*. 2017. Vol. 113, p. 23-35. DOI: 10.1016/j.mineng.2017.07.018
30. Ruiz M.C., Risso J., Seguel J., Padilla R. Solvent extraction of copper from sulfate-chloride solutions using mixed and modified hydroxyoxime extractants. *Minerals Engineering*. 2020. Vol. 146, p.106-109. DOI: 10.1016/j.mineng.2019.106109
31. Shaw D.R., Dreisinger D.B., Lancaster T. et al. The commercialization of the FENIX iron control system for purifying copper electrowinning electrolytes. *JOM*. 2004. Vol. 56. Iss. 7, p. 38-41. DOI: 10.1007/s11837-004-0090-x
32. Sun Y., Chen J., Li X., Myint W. The high sulfidation epithermal copper deposits at Monywa, Central West Myanmar: Poster. SEG-CODES Conference, September 27-30, 2015, Hobart, Australia. SEG, 2015, p. 2.
33. Dong C.-S., Shen Q., Zhang Y.-H. et al. The surface sulphidization and wetting of lead oxide fine particles. *Minerals Engineering*. 2019. Vol. 134, p. 241-249. DOI: 10.1016/j.mineng.2019.02.014

Authors: Kyaw Min Soe, Candidate of Engineering Sciences, kyaw@ipe.ac.cn, <https://orcid.org/0000-0002-2500-5102> (CAS Key Laboratory of Green Process and Engineering, Institute of Process Engineering, Chinese Academy of Sciences, Beijing, People's Republic of China; National Engineering Laboratory for Hydrometallurgical Cleaner Production Technology, Chinese Academy of Sciences, Beijing, People's Republic of China; University of Chinese Academy of Sciences, Beijing, People's Republic of China), **Renman Ruan**, Doctor of Engineering Sciences, Professor, rman@ipe.ac.cn, <https://orcid.org/0000-0001-6304-2644> (CAS Key Laboratory of Green Process and Engineering, Institute of Process Engineering, Chinese Academy of Sciences, Beijing, People's Republic of China; National Engineering Laboratory for Hydrometallurgical Cleaner Production Technology, Chinese Academy of Sciences, Beijing, People's Republic of China; State Key Laboratory of Biochemical Engineering Institute of Process Engineering, Chinese Academy of Sciences, Beijing, People's Republic of China), **Yan Jia**, Doctor of Engineering Sciences, Associate Professor, yjia@ipe.ac.cn, <https://orcid.org/0000-0001-8477-9725> (CAS Key Laboratory of Green Process and Engineering, Institute of Process Engineering, Chinese Academy of Sciences, Beijing, People's Republic of China; National Engineering Laboratory for Hydrometallurgical Cleaner Production Technology, Chinese Academy of Sciences, Beijing, People's Republic of China; State Key Laboratory of Biochemical Engineering Institute of Process Engineering, Chinese Academy of Sciences, Beijing, People's Republic of China), **Qiaoyi Tan**, Master of Engineering Sciences, Senior Researcher, qytan@ipe.ac.cn, <https://orcid.org/0000-0002-7513-9205> (CAS Key



Laboratory of Green Process and Engineering, Institute of Process Engineering, Chinese Academy of Sciences, Beijing, People's Republic of China; National Engineering Laboratory for Hydrometallurgical Cleaner Production Technology, Chinese Academy of Sciences, Beijing, People's Republic of China; State Key Laboratory of Biochemical Engineering Institute of Process Engineering, Chinese Academy of Sciences, Beijing, People's Republic of China), **Zhentang Wang**, Master of Engineering Sciences, Managing Director of Myanmar Yangtze Copper Ltd, wzt@emytcl.com, <https://orcid.org/0000-0002-6307-9962> (Wanbao Mining Ltd, Beijing, People's Republic of China), **Jianfeng Shi**, Master of Engineering Sciences, General Manager of Myanmar Wanbao Mining Ltd, sjf@wbmining.com, <https://orcid.org/0000-0001-6990-5586> (Wanbao Mining Ltd, Beijing, People's Republic of China), **Chuangang Zhong**, Master of Engineering Sciences, Head of Engineering Department, zhongchg@wbmining.com, <https://orcid.org/0000-0003-3892-8085> (Wanbao Mining Ltd, Beijing, People's Republic of China), **Heyun Sun**, Master of Engineering Sciences, Senior Researcher, sunhy@ipe.ac.cn, <https://orcid.org/0000-0001-9090-4780> (CAS Key Laboratory of Green Process and Engineering, Institute of Process Engineering, Chinese Academy of Sciences, Beijing, People's Republic of China; National Engineering Laboratory for Hydrometallurgical Cleaner Production Technology, Chinese Academy of Sciences, Beijing, People's Republic of China; State Key Laboratory of Biochemical Engineering Institute of Process Engineering, Chinese Academy of Sciences, Beijing, People's Republic of China).

The authors declare no conflict of interests.

The paper was received on 10 June, 2020.

The paper was accepted for publication on 1 February, 2021.